



Cite this: *Chem. Commun.*, 2015, 51, 10206

Received 27th April 2015,
Accepted 15th May 2015

DOI: 10.1039/c5cc03517a

www.rsc.org/chemcomm

A one-step, modular route to optically-active diphos ligands†

E. Louise Hazeland, Andy M. Chapman, Paul G. Pringle* and Hazel A. Sparkes

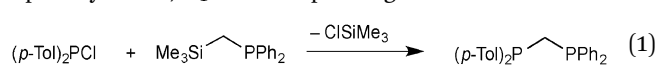
A chlorosilane elimination reaction has been developed that allows the efficient synthesis of optically pure C₁-symmetric, C₁-backboned diphosphines with a wide variety of stereoelectronic characteristics.

Asymmetric hydrogenation, catalyzed by metal complexes of optically active phosphines, was a landmark discovery in chemistry.^{1,2} Numerous diphosphines^{3–9} have been invented for the enantioselective hydrogenation of alkenes, ketones and imines and several have found industrial applications.^{10,11} The diphos ligands **A–F** shown in Fig. 1 represent milestones *en route* to the current understanding of the features that create an effective ligand for asymmetric catalysis and they continue to inspire the design of new ligands.¹²

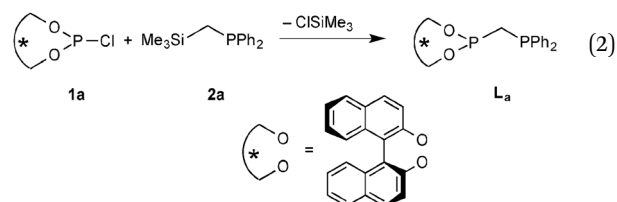
The high enantioselectivity obtained with catalysts based on C₂- or C₁-symmetric diphosphines has been rationalized in terms of the degree of control of the metal binding site offered by the chelates involved.¹³ For example the rigid 4-membered rings formed by the C₁-backboned **E** and **F** (Fig. 1) have been

spectacularly effective for asymmetric hydrogenation,^{7,8,14} and it is the rigidity of the metal chelates that appears to be a critical feature of these catalysts. Despite the multitude of diphos ligands that have been prepared, there continues to be a need for new ones because, as several authors have noted, ligand discovery remains largely an empirical rather than a rational endeavour.¹⁵ A disadvantage of diphos ligands is that their synthesis is often multistep and/or requires an optical resolution step, making systematic refinement of their structures time-consuming and laborious.¹⁶ A major reason why monophos ligands such as **G** have attracted attention¹⁷ is that their synthesis is simple, modular and so reliable that they have been employed in high-throughput experimentation (HTE). Here we report a simple, one-step route to C₁-linked diphos ligands that has the capacity to create a library of optically-active diphos ligands rapidly.

The construction of achiral C₁-linked diphosphines by an Si–P exchange reaction such as that shown in eqn (1) has been previously reported.^{18,19} The attraction of this route is that the volatile by-product is readily removed and therefore we have investigated its potential as the basis for a general route to optically active, C₁-linked diphos ligands.



The reaction of chlorophosphite **1a** with the trimethylsilyl-methyl-phosphine **2a** gave the diphos ligand **L_a** quantitatively (eqn (2)).



The reactants in eqn (2) are readily varied and easily prepared.^{19–22} Thus **L_{b–f}** are produced in high yields from the reactions of trimethylsilylmethylphosphines **2b–d** with the

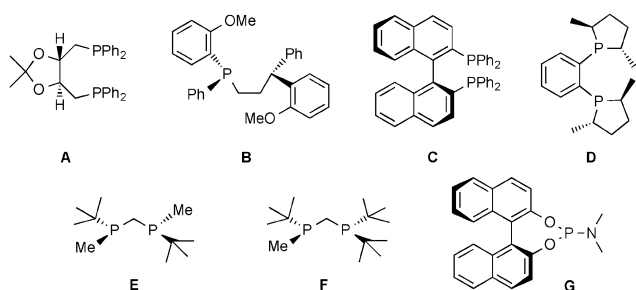


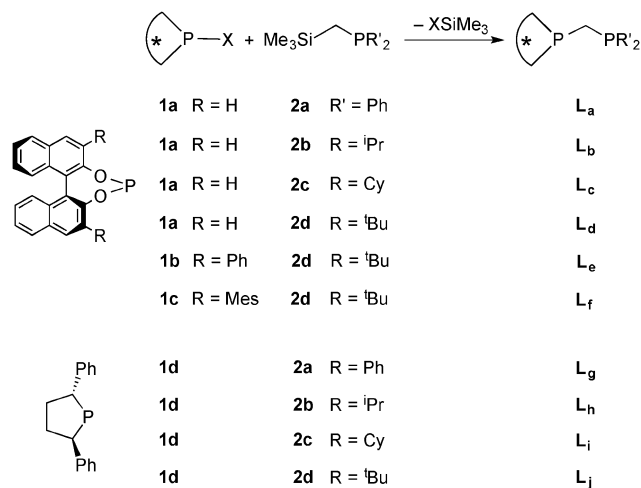
Fig. 1 Phosphorus ligands for asymmetric hydrogenation. **A** = diop,³ **B** = dipamp,⁴ **C** = binap,⁵ **D** = DuPhos,⁶ **E** = miniphos,⁷ **F** = trichicken-footphos,⁸ **G** = monophos.⁹

School of Chemistry, University of Bristol, Cantock's Close, Bristol, BS8 1TS, UK.

E-mail: paul.pringle@bristol.ac.uk

† Electronic supplementary information (ESI) available: Experimental details, additional spectra and crystallographic data. CCDC 1059329 and 1059330. For ESI and crystallographic data in CIF or other electronic format see DOI: 10.1039/c5cc03517a

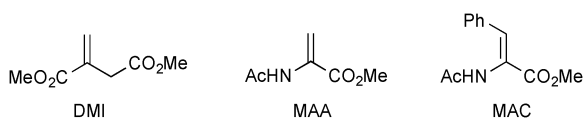




Scheme 1 Synthesis of the diphos ligands **L_{a-j}**. X = Cl in all cases except for **1b** and **1c** where X = Br.

corresponding optically-pure halophosphites **1a–c** (Scheme 1). A significant extension of this process was achieved by employing the optically pure chlorophosphacycle **1d** (Scheme 1) to produce **L_{g-j}**. The crude products **L_{a-j}** were sufficiently pure to be used in catalysis without further purification.

The complexes [Rh(diene)L] (**3**) where diene = 1,5-cyclooctadiene or norbornadiene were generated by the addition of **L_{a-j}** to [Rh(diene)₂][BF₄] in CH₂Cl₂ and in each case the product was identified from the characteristic AMX pattern in its ³¹P NMR spectrum (see ESI† for details). Representative examples of **3**, where L = **L_d** or **L_{g-j}**, have been isolated and fully characterised. The ligands were screened for the asymmetric hydrogenation of the three benchmark substrates DMI, MAA and MAC (structures shown below) and the results are given in Table 1 and depicted graphically in Fig. 2 from which it is clear that significant variation in selectivity occurs for ostensibly small changes in ligand structure.



For the complexes of the binol-derived **L_{a-d}** with DMI and MAA, the highest ee was obtained with the PCy₂ derivative: **L_a** < **L_b** < **L_c** > **L_d** (entries 1–12 in Table 1). For the complexes of the 3,3'-substituted ligands **L_{d-f}**, the highest ee was obtained when the 3,3'-substituents were Ph: **L_d** < **L_e** > **L_f** (entries 10–18 in Table 1). With complexes of the phospholane-derived ligand **L_{g-j}**, the enantioselectivity was greatest for the P^tBu₂ ligand: **L_g** < **L_h** < **L_i** < **L_j** (entries 19–30). It is apparent from Fig. 2 that the performance of any particular ligand can be highly substrate-dependent.

The absolute configuration of the asymmetric hydrogenation products obtained with Rh-diphos complexes generally obey the quadrant-blocking rule; that is, blocked upper left quadrant leads to *R*-configuration for MAC and MAA and *S*-configuration for DMI.¹³ The nature of the quadrant blocking is best discerned

Table 1 Asymmetric hydrogenation catalysis^a

Entry	Ligand	DMI	MAA	MAC	Conv. (%)
1	L_a	68 (<i>S</i>)			100
2	L_a		46 (<i>R</i>)		100
3	L_a			35 (<i>R</i>)	100
4	L_b	90 (<i>S</i>)			100
5	L_b		72 (<i>R</i>)		100
6	L_b			56 (<i>R</i>)	100
7	L_c	95 (<i>S</i>)			100
8	L_c		76 (<i>R</i>)		100
9	L_c			61 (<i>R</i>)	100
10	L_d	91 (<i>S</i>)			100
11	L_d		65 (<i>R</i>)		100
12	L_d			64 (<i>R</i>)	100
13	L_e	94 (<i>S</i>)			56
14	L_e		98 (<i>R</i>)		100
15	L_e			94 (<i>R</i>)	49
16	L_f	91 (<i>S</i>)			47
17	L_f		72 (<i>R</i>)		35
18	L_f			93 (<i>R</i>)	20
19	L_g	62 (<i>R</i>)			100
20	L_g		57 (<i>S</i>)		100
21	L_g			46 (<i>S</i>)	99
22	L_h	97 (<i>R</i>)			100
23	L_h		90 (<i>S</i>)		100
24	L_h			85 (<i>S</i>)	39
25	L_i	92 (<i>R</i>)			100
26	L_i		96 (<i>S</i>)		100
27	L_i			85 (<i>S</i>)	22
28	L_j	99 (<i>R</i>)			100
29	L_j		98 (<i>S</i>)		100
30	L_j			99 (<i>S</i>)	26

^a Reaction conditions: S/C = 100:1, 5 bar H₂, 20 °C, 1 h, CH₂Cl₂. Enantioselectivities were determined by chiral GC analysis (see ESI† for details).

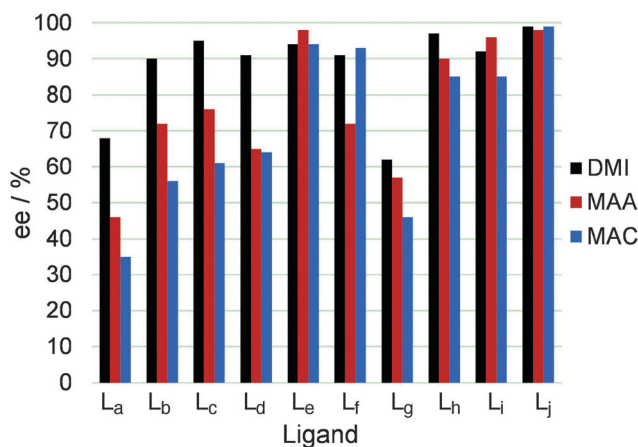


Fig. 2 Graph of the enantioselectivities obtained with each of the catalysts.

from crystal structures and so crystals of the [Rh(cod)(**L_j**)]BF₄ (**3j**) were grown and its crystal structure determined, which has two molecules in the asymmetric unit (Fig. 3). Attempts to grow crystals suitable for X-ray crystallography of Rh-complexes of the binol-derived ligands (**L_{a-d}**) have so far been unsuccessful, although crystals of the chelate [PtCl₂(**L_d**)] (**4d**) have been obtained and its structure is shown in Fig. 4. In both structures (**3j** and **4d**), the acute P–M–P angles of 72.84(3)° in **3j** and 73.74(3)° in **4d** indicate the degree of strain present in the 4-membered chelates; these values are very similar to the 72.55(6)° that was



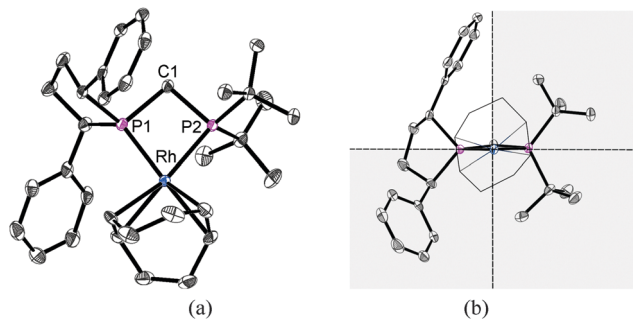


Fig. 3 (a) Crystal structure of **3j**. Thermal ellipsoids are plotted at 50% probability. Hydrogen atoms and the BF_4 counterion have been omitted for clarity. The two molecules in the asymmetric unit have the same orientation hence only one is shown for clarity. Selected bond lengths (Å) and angles ($^\circ$): Rh1–P1 2.2839(7), Rh1–P2 2.3198(7), P1–C1 1.841(3), P2–C1 1.846(3), P1–Rh1–P2 72.84(3), P1–C1–P2 95.68(13). (b) Quadrant diagram of **3j**, where shaded area represents a blocked quadrant.

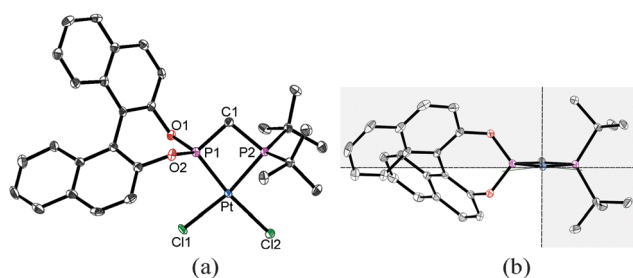
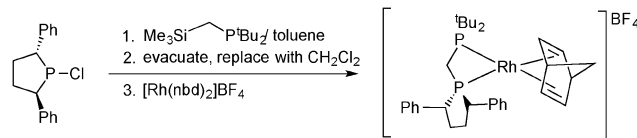


Fig. 4 (a) Crystal structure of **4d**. Thermal ellipsoids are plotted at 50% probability. Hydrogen atoms have been omitted for clarity. Selected bond lengths (Å) and angles ($^\circ$): Pt–C1 2.3572(8), Pt–C2 2.3657(8), Pt–P1 2.1620(9), Pt–P2 2.2596(8), P1–C1 1.798(3), P2–C1 1.866(3), P1–Pt–P2 73.74(3), P1–C1–P2 92.83(15), O1–P1–O2 104.26(13). (b) Quadrant diagram of **4d**, where shaded area represents a blocked quadrant.

determined in an analogous complex of Trichickenfootphos (**F** in Fig. 1).⁸ The mean planes through M–P–C have rms deviations of 0.035/0.049 Å in **3j** and 0.003 Å in **4d** showing that the chelates are almost planar (see Fig. 3 and 4). It is evident from Fig. 4 that the upper left quadrant is blocked in the L_d complex (and presumably the same would be the case for all the ligands L_{a-f}) while Fig. 3 shows lower left quadrant is blocked in the L_j complex (and presumably the same would be the case for all the ligands L_{g-j}). Therefore, the absolute configurations of the products of asymmetric hydrogenation (Table 1) conform to the quadrant rule.

The remarkable efficiency of the ligand synthesis (Scheme 1) coupled with the ready removal of the volatile chlorosilane by-product suggested that a one-pot procedure may be feasible. This was carried out according to Scheme 2 for L_j and the product tested for asymmetric hydrogenation of MAA. The 97% ee that was obtained compares favourably with the 98% ee recorded with the isolated complex (Table 1).

The simplicity and generality of the chlorosilane elimination route shown in Scheme 1 to C_1 -symmetric, C_1 -backboned, optically pure diphos ligands has been demonstrated by varying the nature of the two P-reagents. The success of the one-pot procedure (Scheme 2), coupled with the fact that the number of



Scheme 2 One pot synthesis of $[\text{Rh}(\text{nbd})(\text{L}_j)]$.

potential ligands increases geometrically with each new chlorophos or silylmethylphosphine component, opens up the possibility of applying HTE methods to diphosphine synthesis and catalyst screening in a way that previously, have only been applied to monophos ligands. This is currently under investigation as is the mechanism of the ligand formation reaction.

We thank EPSRC for supporting this work with a studentships to ELH.

Notes and references

- W. S. Knowles and M. J. Sabacky, *Chem. Commun.*, 1968, 1445–1446.
- L. Horner, H. Siegel and H. Büthe, *Angew. Chem., Int. Ed. Engl.*, 1968, 7, 942.
- T. P. Dang and H. B. Kagan, *J. Chem. Soc. D*, 1971, 481.
- W. S. Knowles, M. J. Sabacky, B. D. Vineyard and D. J. Weinkauff, *J. Am. Chem. Soc.*, 1975, 97, 2567–2568.
- A. Miyashita, A. Yasuda, H. Takaya, K. Toriumi, T. Ito, T. Souchi and R. Noyori, *J. Am. Chem. Soc.*, 1980, 102, 7932–7934.
- M. J. Burk, *J. Am. Chem. Soc.*, 1991, 113, 8518–8519.
- Y. Yamanoi and T. Imamoto, *J. Org. Chem.*, 1999, 64, 2988–2989.
- G. Hoge, H.-P. Wu, W. S. Kissel, D. A. Pflum, D. J. Greene and J. Bao, *J. Am. Chem. Soc.*, 2004, 126, 5966–5967.
- M. van den Berg, A. J. Minnaard, E. P. Schudde, J. van Esch, A. H. M. de Vries, J. G. de Vries and B. L. Feringa, *J. Am. Chem. Soc.*, 2000, 122, 11539–11540.
- J. G. de Vries and C. J. Elsevier, *The Handbook of Homogeneous Hydrogenation*, Wiley-VCH, 2008.
- C. Jäkel and R. Paciello, *US Patent*, 2008/269528, 2008.
- (a) J. A. Gillespie, D. L. Dodds and P. C. J. Kamer, *Dalton Trans.*, 2010, 39, 2751–2764; (b) G. M. Noonan, J. A. Fuentes, C. J. Cobley and M. L. Clarke, *Angew. Chem., Int. Ed.*, 2012, 51, 2477–2480; (c) X. Wang, F. Meng, Y. Wang, Z. Han, Y.-J. Chen, L. Liu, Z. Wang and K. Ding, *Angew. Chem., Int. Ed.*, 2012, 51, 9276–9282; (d) T. Imamoto, K. Tamura, Z. Zhang, Y. Horiuchi, M. Sugiya, K. Yoshida, A. Yanagisawa and I. D. Gridnev, *J. Am. Chem. Soc.*, 2012, 134, 1754–1769; (e) S. H. Chikkali, R. Bellini, B. de Bruin, J. I. van der Vlugt and J. N. H. Reek, *J. Am. Chem. Soc.*, 2012, 134, 6607–6616; (f) N. Khiri-Meribout, E. Bertrand, J. Bayardon, M.-J. Eymyn, Y. Roussel, H. Cattey, D. Fortin, P. D. Harvey and S. Jugé, *Organometallics*, 2013, 32, 2827–2839; (g) A. Zirakzadeh, M. A. Groß, Y. Wang, K. Mereiter, F. Spindler and W. Weissensteiner, *Organometallics*, 2013, 32, 1075–1084; (h) W. Chen, F. Spindler, B. Pugin and U. Nettekoven, *Angew. Chem., Int. Ed.*, 2013, 52, 8652–8656; (i) A. Zirakzadeh, M. A. Groß, Y. Wang, K. Mereiter and W. Weissensteiner, *Organometallics*, 2014, 33, 1945–1952; (j) G. Shang, W. Li and X. Zhang, *Catalytic Asymmetric Synthesis*, John Wiley & Sons, Inc., 2010, pp. 343–436.
- I. D. Gridnev and T. Imamoto, *Acc. Chem. Res.*, 2004, 37, 633–644.
- I. D. Gridnev, T. Imamoto, G. Hoge, M. Kouchi and H. Takahashi, *J. Am. Chem. Soc.*, 2008, 130, 2560–2572.
- (a) A. H. Hoveyda, A. W. Bird and M. A. Kacprzynski, *Chem. Commun.*, 2004, 1779–1785; (b) J. G. de Vries and L. Lefort, *Chem. – Eur. J.*, 2006, 12, 4722–4734; (c) W. Zhang, Y. Chi and X. Zhang, *Acc. Chem. Res.*, 2007, 40, 1278–1290.
- R. den Heeten, B. H. G. Swennenhuis, P. W. N. M. van Leeuwen, J. G. de Vries and P. C. J. Kamer, *Angew. Chem., Int. Ed.*, 2008, 47, 6602–6605.
- (a) L. Lefort, J. A. F. Boogers, A. H. M. de Vries and J. G. de Vries, *Org. Lett.*, 2004, 6, 1733–1735; (b) L. Lefort, J. A. F. Boogers, A. H. M. de Vries and J. G. de Vries, *Top. Catal.*, 2006, 40, 185–191.
- (a) R. Appel, K. Geisler and H. F. Scholer, *Chem. Ber./Recl.*, 1979, 112, 648–653; (b) J. Wolf, M. Manger, U. Schmidt, G. Fries, D. Barth,



- B. Weberndorfer, D. A. Vicić, W. D. Jones and H. Werner, *J. Chem. Soc., Dalton Trans.*, 1999, 1867–1875; (c) R. L. Keiter, D. Chen, G. A. Holloway, E. A. Keiter, Y. Zang, M. T. Huml, J. Filley and D. E. Brandt, *Organometallics*, 2012, **31**, 4619–4622.
- 19 J. Campora, C. M. Maya, I. Matas, B. Claasen, P. Palma and E. Alvarez, *Inorg. Chim. Acta*, 2006, **359**, 3191–3196.
- 20 A. S. Ionkin, Y. Wang, W. J. Marshall and V. A. Petrov, *J. Organomet. Chem.*, 2007, **692**, 4809–4827.
- 21 M. J. Baker and P. G. Pringle, *J. Chem. Soc., Chem. Commun.*, 1991, 1292–1293.
- 22 P. Haranath, U. Anasuyamma, C. Devendranath Reddy and C. Suresh Reddy, *Heterocycl. Commun.*, 2005, **11**, 335–342.

